Device Physics of OLEDs

2009. 5.28.

Changhee Lee
School of Electrical Engineering and Computer Science
Seoul National Univ.
chlee7@snu.ac.kr

Advantages of OLEDs

- Simple fabrication processes:
  vacuum deposition, inkjet printing, spin coating, roll-to-roll (web) processing
- Superior viewing performance:
  emissive bright colors, wide viewing angle, fast response time, and high contrast
- Excellent operating characteristics:
  low operating voltage, power efficient, and wide temperature range
- Good form factor:
  Thin, light-weight, rugged, and flexible

→ Ultimate Portable Communication Devices

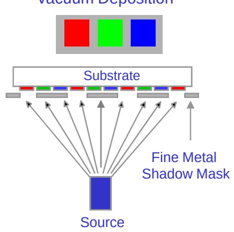

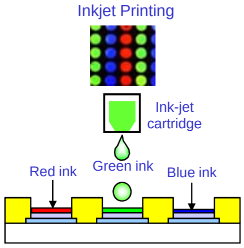

http://www.universaldisplay.com/

OLED vs LCD
(http://www.oled-display.net/oled-television)

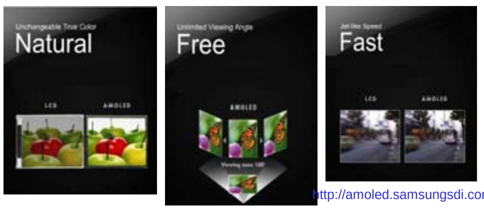

http://amoled.samsungsdi.com/

Development of OLED technology

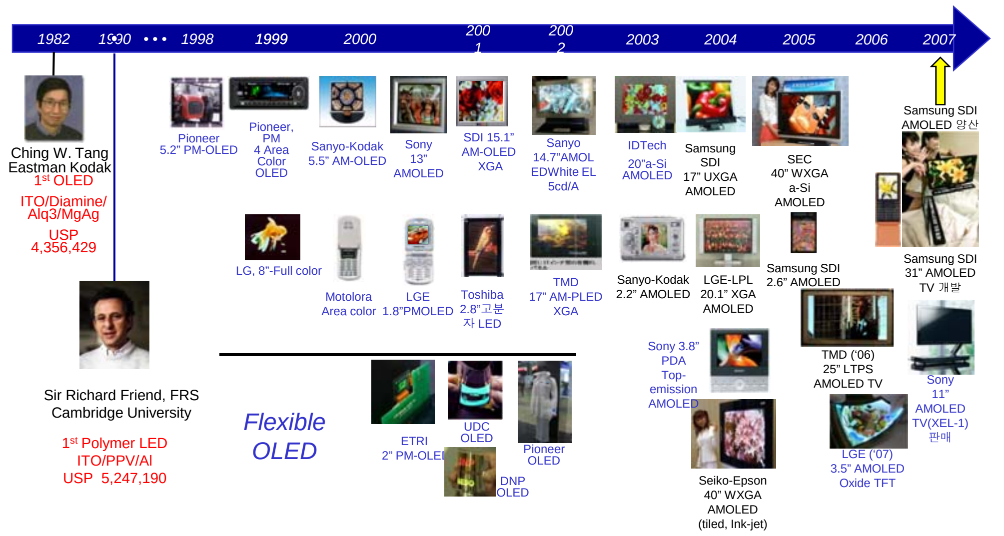

Progress in the efficiency of white OLEDs

Organic Semiconductor
EE 4541.617A
2009. 1st Semester

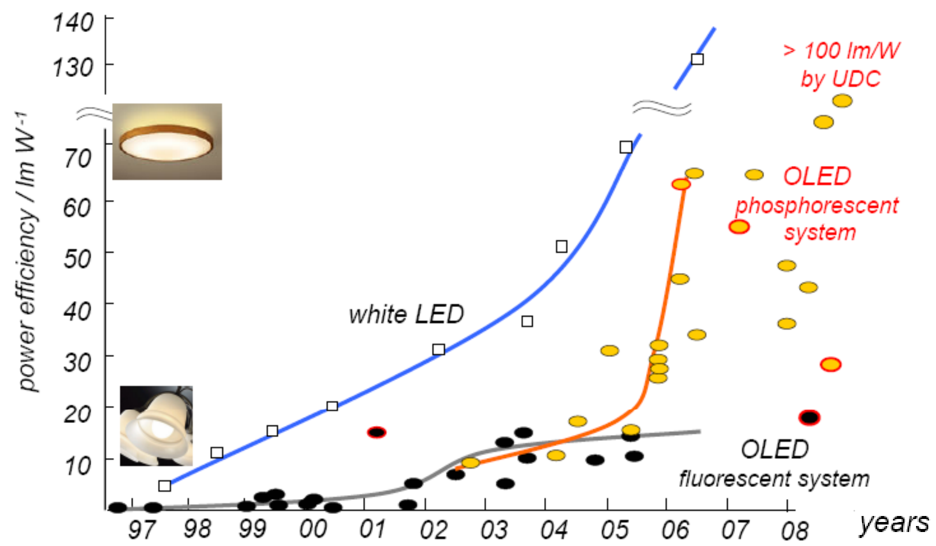

N. Ide (Matsushita Electric Works, Ltd.), et al., SPIE (2008)

Changhee Lee, SNU, Korea

Organic LEDs (*polymers or small molecules*)

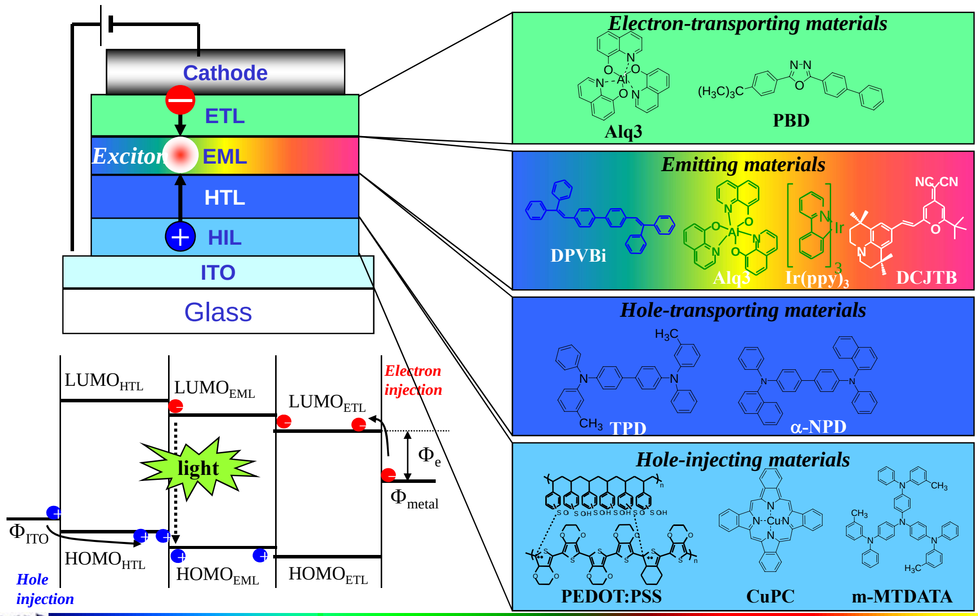

Fluorescent emitters

	B	G	Y	R
Host	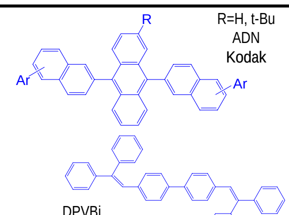 R=H, t-Bu ADN Kodak; DPVBi Idemitsu Kosan	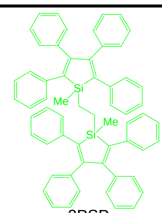 2PSP Chisso	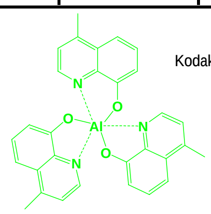 Kodak; Almq3	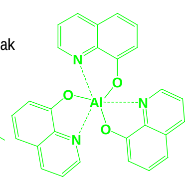 Alq3
Dopant	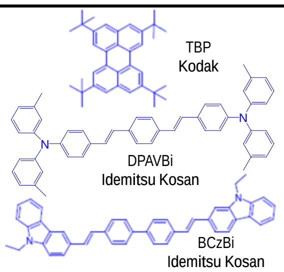 TBP Kodak; DPAVBi Idemitsu Kosan; BCzBi Idemitsu Kosan	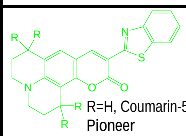 R=H, Coumarin-545 Pioneer; R=CH$_3$, Coumarin-545T Kodak; 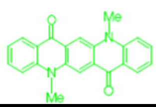 Me-QA Pioneer	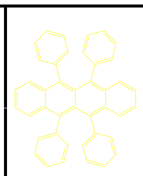 rubrene Mitsubishi	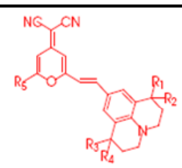 R$_1$=R$_2$=R$_3$=R$_4$=H, R$_5$=Me DCM-2; R$_1$=R$_2$=R$_3$=R$_4$=Me, R$_5$=t-Bu DCJTB Kodak

Host and Phosphorescent Dopant Materials

	Blue	Green	Red
Dopant	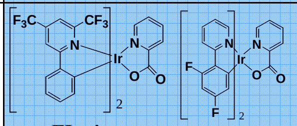 **FIrpic** **$(CF_3ppy)_2Ir(pic)$**	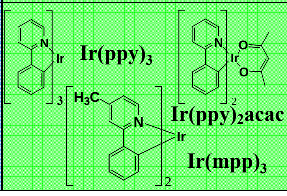 **$Ir(ppy)_3$** **$Ir(ppy)_2acac$** **$Ir(mpp)_3$**	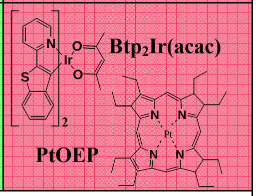 **$Btp_2Ir(acac)$** **PtOEP**
Host	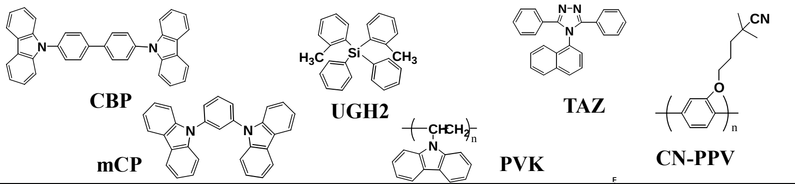 **CBP** **mCP** **UGH2** **PVK** **TAZ** **CN-PPV**		
Hole/Exciton Blocking Materials	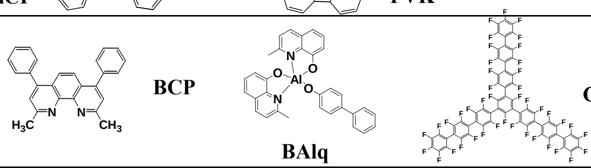 **BCP** **BAlq** **$C_{60}F_{42}$**		

Dr. H. N. Cho (InkTek)

Comparison of fluorescent and phosphorescent OLEDs

	Fluorescence	**Phosphorescence**
Host	Alq3, ...	CBP, TCTA, mCP, …
Excited state	Singlet	Triplet
Exciton diffusion length	50 ~ 100 Å	> 1000 Å
Exciton blocking layer	-	BCP, Balq, etc.
Dopant concentration	0.1 ~ 3 %	5 – 15 %
Maximum quantum efficiency	25 %	100 %
Luminous efficacy	Red: ~6 cd/A Green: ~20 cd/A Blue: ~6 cd/A	Red: 6~20 cd/A Green: 17~50 cd/A Blue: ~ 10 cd/A
Lifetime	~ 50,000 hour	~10,000 hour

OLED Performance

Color			CIE (x,y)	Efficiency (cd/A)	Half-Life (hr)
저분자	형광	Red	0.65, 0.35	5.5	>80,000 @ 1000 cd/m^2
		Green	0.32, 0.62	19	40,000 @ 1000 cd/m^2
		Light blue	0.17, 0.30	12	21,000 @ 1000 cd/m^2
		Blue	0.15, 0.15	5.9	7,000 @ 1000 cd/m^2
		White	0.30, 0.34	12	23,000 @ 1000 cd/m^2
	인광	Red	0.65, 0.35	15	>22,000 @ 500 cd/m^2
		Orange	0.61, 0.38	22	15,000 @ 300 cd/m^2
		Green	0.31, 0.64	27	25,000 @ 600 cd/m^2
		Light blue	0.14, 0.23	8	-
		White	0.39, 0.39	38	-
고분자	형광	Red	0.68, 0.32	1.7	1790 @ 1000 cd/m^2
		Orange	0.58, 0.42	0.9	8138 @ 1000 nit
		Yellow	0.50, 0.49	2.1	2420 @ 4000 cd/m^2
		Green	0.43, 0.55	7.7	2912 @ 2000 cd/m^2
		Blue	0.16, 0.22	6.9	>1147 @ 800 cd/m^2
		White	0.30, 0.33	3.8	235 @ 800 cd/m^2
	인광	Red	0.67, 0.28	1.3	>8350 @ 100 cd/m^2
		Green	0.36, 0.59	22.8	2649 @ 400 cd/m^2

Electron-Hole Balance

- Electron-Hole Balance → improved efficiency & Lifetime

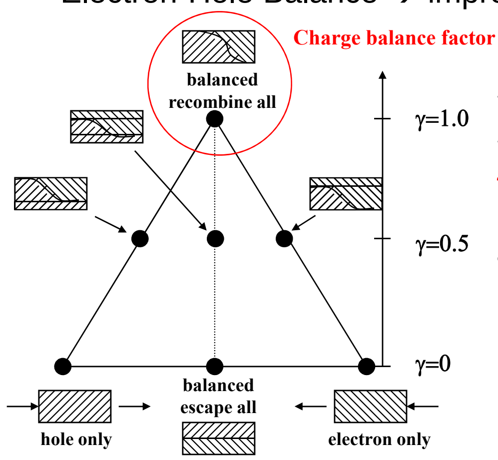

J. C. Scott et al., SPIE Proc., 3476, 111 (1998)

$$\eta_\phi = \chi\gamma\beta\phi_L$$

χ:coupling-out factor

γ:charge balance factor

β:probability of production of emissive species

ϕ_L:quantum efficiency of luminescence

To maximize the charge balance factor γ:
- Equal amount of electrons and holes are injected.
- All the injected electrons and holes recombine.

→ Ambipolar emitting layer
→ Mixed emitting layer (co-doped host)
→ p-type or n-type doping at the electrode interface

Electron injection layer

Enhanced electron injection in OLEDs using an Al/LiF electrode

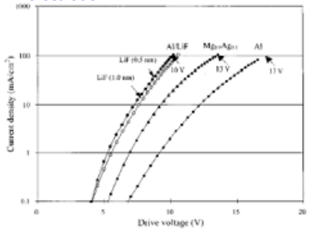

FIG. 1. Current–voltage characteristics of three EL devices using an Al, a $Mg_{0.9}Ag_{0.1}$, and an Al/LiF electrode, respectively.

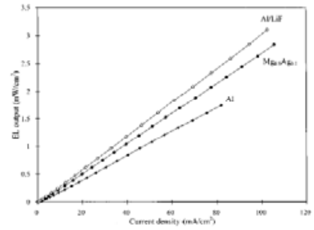

FIG. 3. Light-current characteristics of three EL devices using Al, $Mg_{0.9}Ag_{0.1}$, and Al/LiF electrodes, respectively.

L. S. Hung, C. W. Tang, and M. G. Mason, APL **70**, 152, (1997)

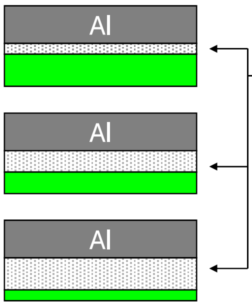

Metal-doped organic layer (n-doping)

Control of:
- Dopant concentration (Extent of reaction)
- Thickness of doped layer

- Realize ohmic contact
- Increase conductivity

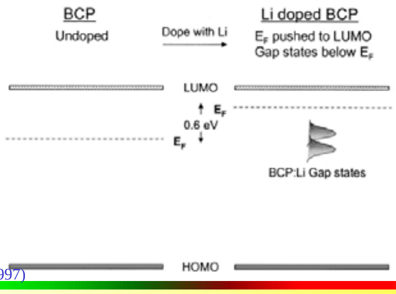

J.Kido et al., Appl.Phys.Lett.(1998)

Hole injection layer (p-doped organic layer)

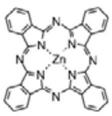

ZnPC

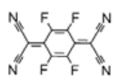

F_4TCNQ

(a)

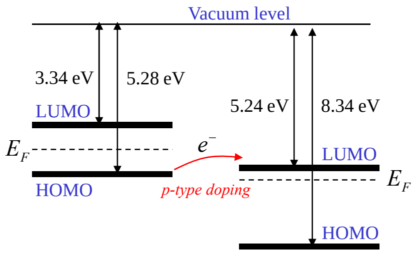

(b)

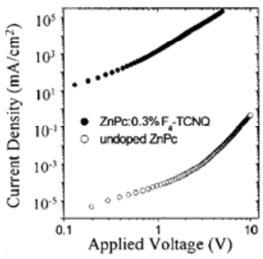

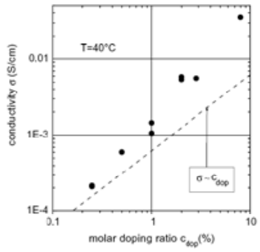

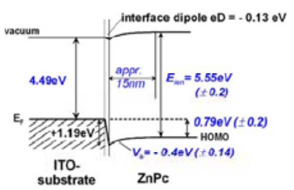

(a) undoped

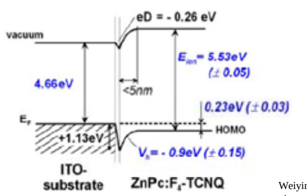

(b) p-type doped

Weiying Gao and Antoine Kahn, Appl. Phys. Lett. 79, 4040 (2001)
zinc phthalocyanine (ZnPc) doped with tetrafluorotetracyanoquinodimethane

M. Pfeiffer , K. Leo, X. Zhou, J.S. Huang, M. Hofmann, A. Werner, J. Blochwitz-Nimoth, Organic Electronics 4 (2003) 89–103

p-i-n OLED

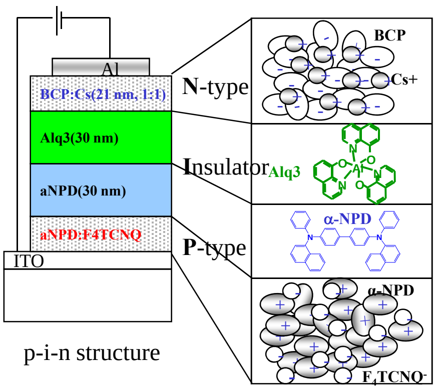

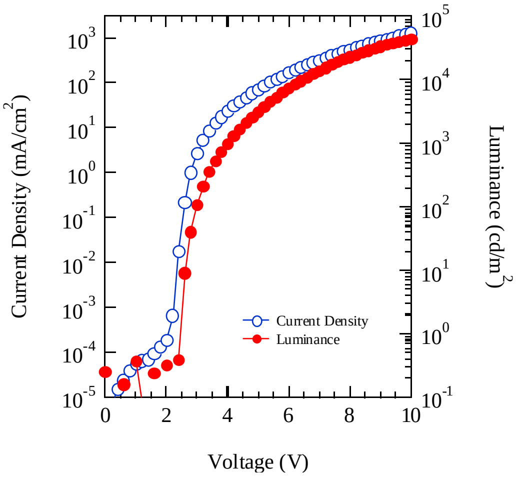

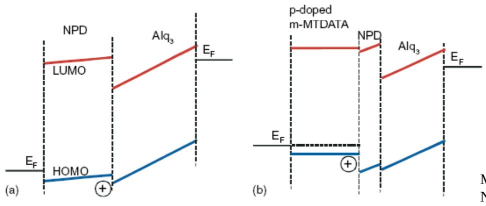

M. Pfeiffer , K. Leo, X. Zhou, J.S. Huang, M. Hofmann, A. Werner, J. Blochwitz-Nimoth, Organic Electronics 4 (2003) 89–103

Tandem OLED

US 20080030131 (2008.02.07) Francisco J. Duarte, Kathleen M. Vaeth, Liang-Sheng Liao, Eastman Kodak Company

A light-emitting device, comprising: a multi-layer stack of materials supported on an optically transparent support member, a first spatial filter, and a second spatial filter spaced from the first spatial filter. The multi-layer stack including at least one organic light-emitting layers, an anode layer, and a cathode layer. The first spatial filter is disposed intermediate the multi-layer stack of materials and the second spatial filter.

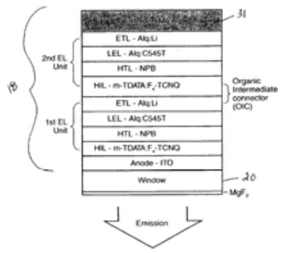

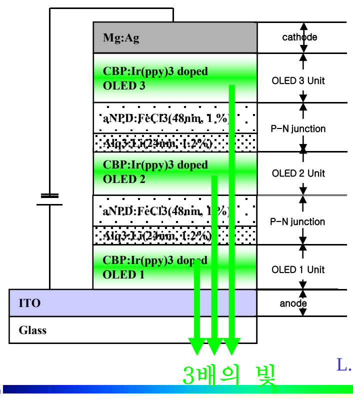

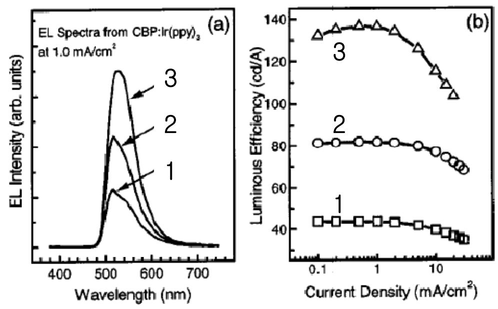

L. S. Liao, K. P. Klubek, and C. W. Tang, Appl. Phys. Lett. **84**, 167 (2004)

I-V characteristics of organic semiconductors

Current
- Injection limited
  - Thermionic emission
    $$J = J_s[\exp(\frac{eV}{k_B T}) - 1] \quad J_s = A^* T^2 \exp(\frac{-e\phi_{bn}}{k_B T})$$
  - Tunneling
    $$J \approx E^2 \exp(\frac{-b}{E}) \quad b = \frac{8\pi\sqrt{2m^*}(q\phi)^{3/2}}{3qh}$$
- Bulk Limited
  - Ohmic (Doped semiconductor)
    $$J = ep\mu E$$
  - SCLC (undoped semicond. or Insulator)
    $$J_{SCLC} = \frac{9}{8}\varepsilon_o \varepsilon_r \mu \frac{V^2}{d^3}$$

Thermionic Emission into low mobility organic semiconductor

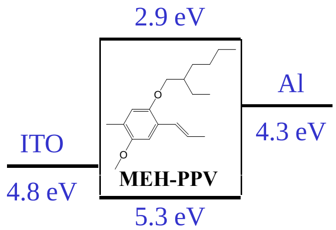

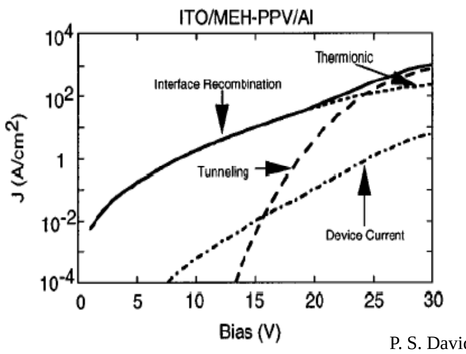

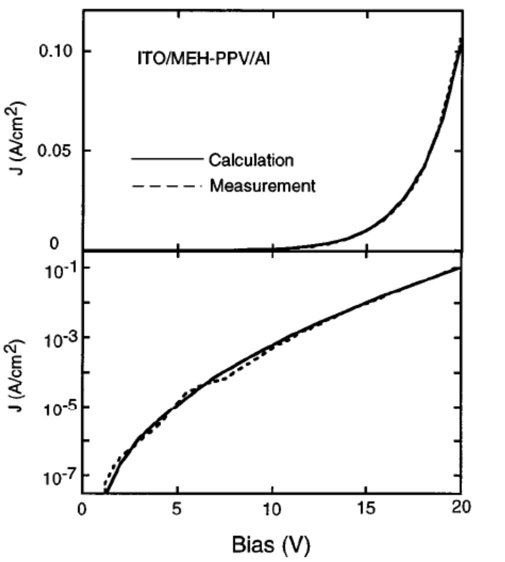

P. S. Davids, I. H. Campbell, and D. L. Smith, J. Appl. Phys. **82**, 6319 (1997).

Tunneling mechanism

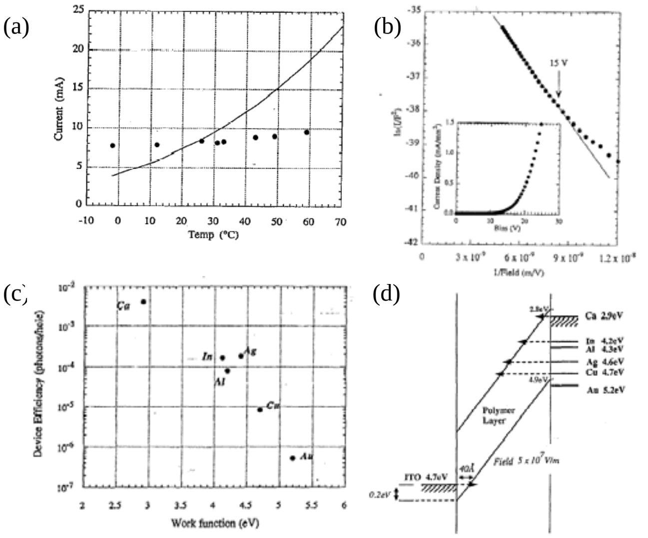

FIG. 10. Device efficiency vs cathode work function for ITO/MEH-PPV devices.

FIG. 11. Band diagram (in forward bias) for model, indicating position of Fermi level for various electrode materials.

I. D. Parker, J. Appl. Phys. **75**, 1656 (1994).

Space-charge-limited (SCL) current

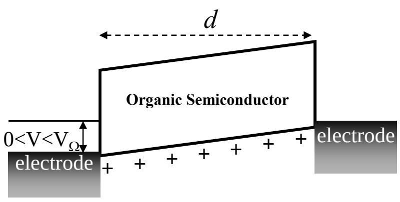

(a) $\tau_t > \tau_d$ (Ohmic current)

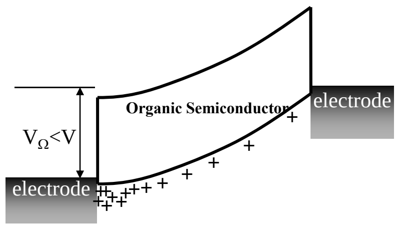

(b) $\tau_t < \tau_d$ (SCL current)

At $\tau_t > \tau_d$, ohmic conduction is predominant.
At $\tau_t < \tau_d$, SCLC conduction is predominant.

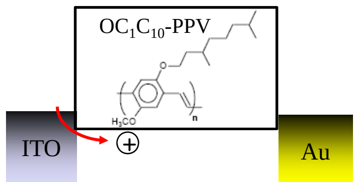

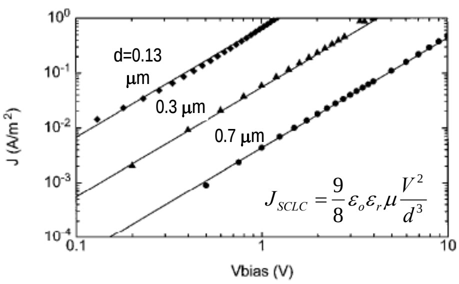

$$J_{SCLC} = \frac{9}{8}\varepsilon_o \varepsilon_r \mu \frac{V^2}{d^3}$$

P. W. M. Blom M. J. M. de Jong, and J. J. M. Vleggaar, Appl. Phys. Lett. 68, 3308 (1996).

Field-dependent mobility in SCL current

$$J_{SCLC} = \frac{9}{8}\varepsilon_o \varepsilon_r \mu \frac{V^2}{d^3} \exp[\frac{0.891}{k_B T} \beta_{PF} (\frac{V}{d})^{1/2}]$$

P. N. Murgatroyd, J. Phys. D: Appl. Phys. **3**, 151 (1970).

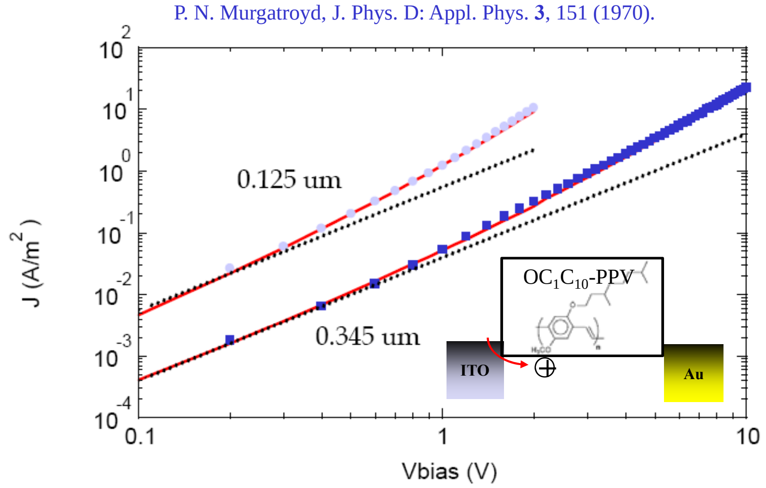

P. W. M. Blom, M. J. M. de Jong, and M. G. van Munster, Phys. Rev. B 55, R656 (1997).

Space-charge-limited (SCL) current

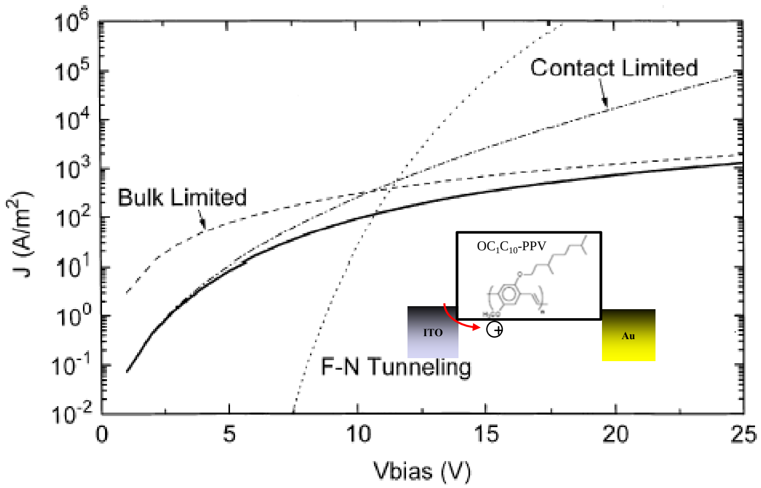

Poly(dialkoxy-p-phenylene vinylene) (OC_1C_{10}-PPV)

P. W. M. Blom M. J. M. de Jong, and J. J. M. Vleggaar, Appl. Phys. Lett. 68, 3308 (1996).

SCL current with an exponential trap distribution

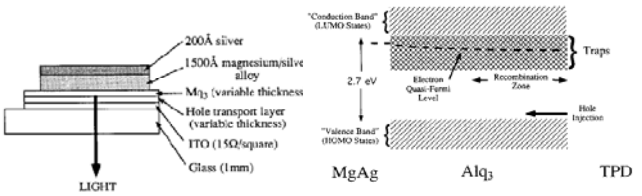

Trap-limited SCLC

$$J \propto \mu N_v N_t^{-m} \frac{V^{m+1}}{d^{2m+1}}, \quad m = \frac{T_t}{T}.$$

$$E_t \approx 0.15\,\mathrm{eV}$$

$$N_t \approx 10^{18}\ \mathrm{cm^{-3}}$$

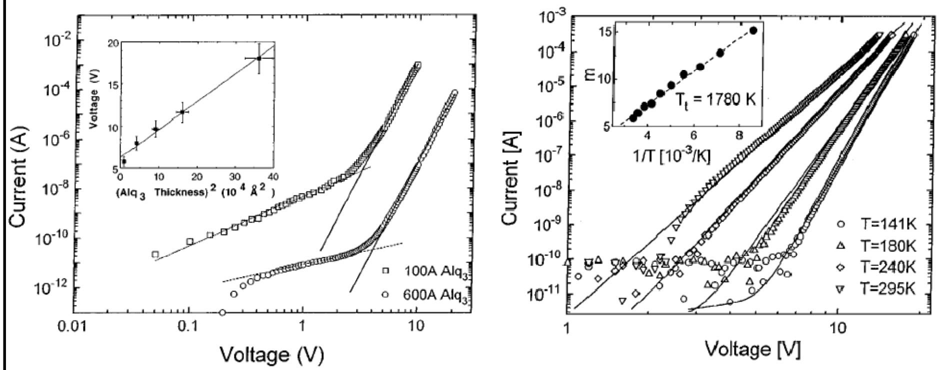

P. E. Burrows, Z. Shen, V. Bulovic, D. M. McCarty, S. R. Forrest, J. A. Cronin and M. E. Thompson, J. Appl. Phys. **79**, 7991 (1996).

Interface-limited injection model

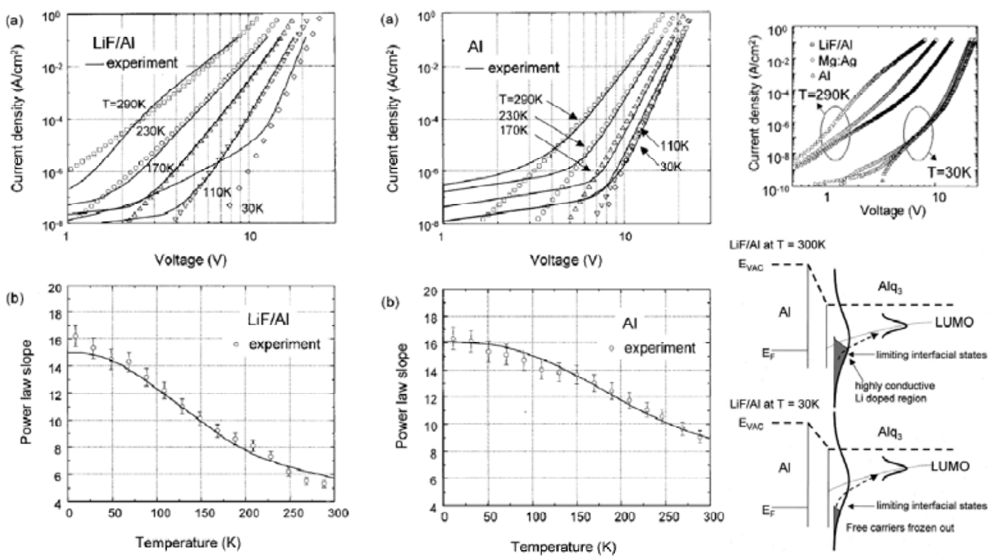

M. A. Baldo and S. R. Forrest, Phys. Rev. B **64**, 085201 (2001)

Carrier Recombination

Recombination of electron hole pairs

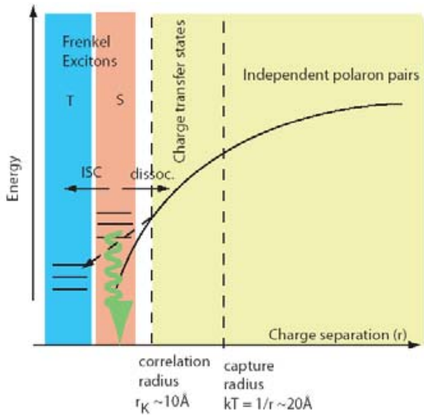

Singlet exciton S=0

$$|\chi_1\chi_2\rangle = \frac{1}{\sqrt{2}}(|\uparrow\downarrow\rangle - |\downarrow\uparrow\rangle)$$

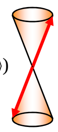

Spin-allowed transition
fast, efficient
Fluorescence

Singlet exciton S=0

Triplet exciton S=1

$$|\chi_1\chi_2\rangle = |\uparrow\uparrow\rangle$$

$$|\chi_1\chi_2\rangle = \frac{1}{\sqrt{2}}(|\uparrow\downarrow\rangle + |\downarrow\uparrow\rangle)$$

$$|\chi_1\chi_2\rangle = |\downarrow\downarrow\rangle$$

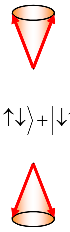

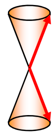

Spin-forbidden transition
slow, inefficient
Phosphorescence

Triplet exciton S=1

M. Segel, M. A. Baldo, R. J. Holmes, S. R. Forrest, Z. G. Soos, Phys. Rev. B 68, 075211 (2003)

Exciton Recombination Zone

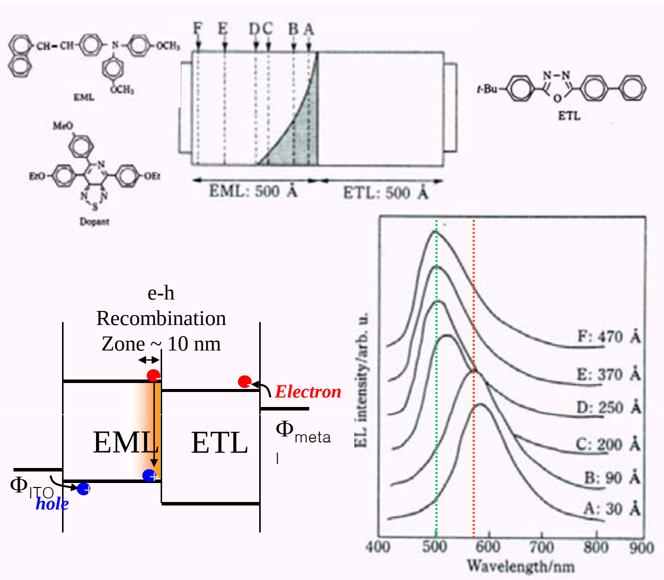

C. Adachi, T. Tsutsui, and S. Saito, *Optoelectron. Devices Technol. 6, 25 (1991).*

Electron-hole and electric field distribution

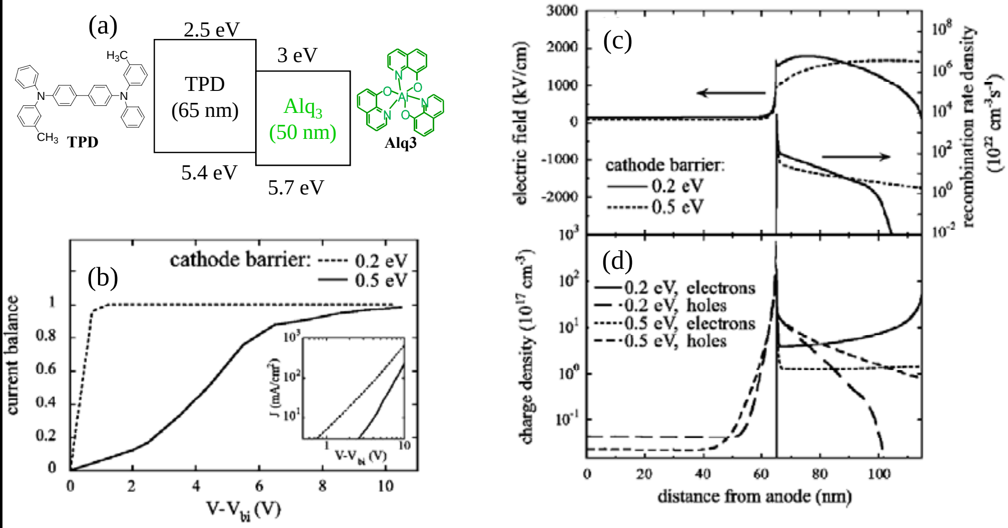

B. Ruhstaller, S. A. Carter, S. Barth, H. Riel, W. Riess, and J. C. Scott, J. Appl. Phys. **89**, 4575 (2001).

Organic Semiconductor
EE 4541.617A
2009. 1st Semester

Quantum efficiency roll-off at high current

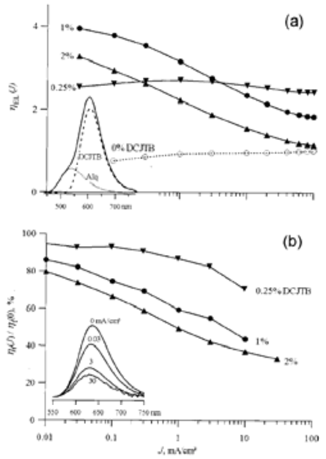

∗ Polaron - exciton quenching :

$$S_1, T_1 \xrightarrow{X^+ \text{ or } X^-} S_0$$

∗ Electric field dissociation of excitons :

$$S_1, T_1 \xrightarrow{\text{E-field}} X^+, X^-$$

J. Szmytkowski, W. Stampor, J. Kalinowski and Z. H. Kafafi, Appl. Phys. Lett. 80, 1465 (2002)

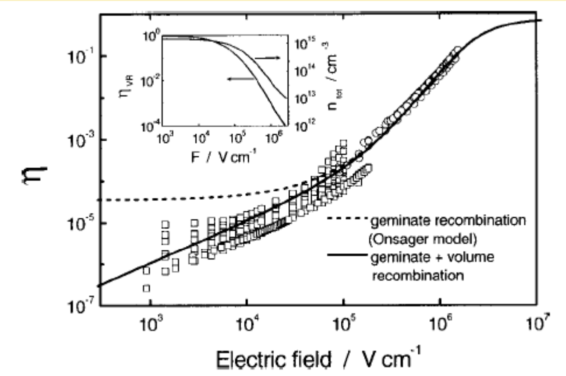

Ralph H. Young, Ching W. Tang, and Alfred P. Marchetti, Appl. Phys. Lett. 80, 874 (2002)

Quantum Efficiency *vs* Current of phosphorescent OLEDs

Triplet – Triplet (T – T) Annihilation

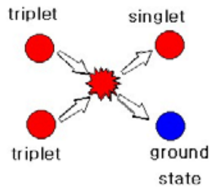

$$\frac{\eta}{\eta_0} = \frac{qd}{2k_T\tau^2 J}\left[-1+\sqrt{1+\frac{8J}{J_T}}\right] = \frac{J_T}{4J}\left[-1+\sqrt{1+\frac{8J}{J_T}}\right]$$

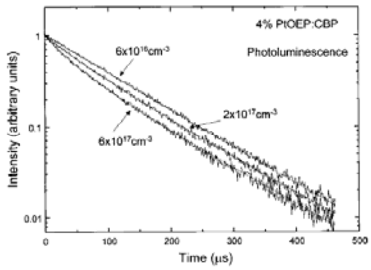

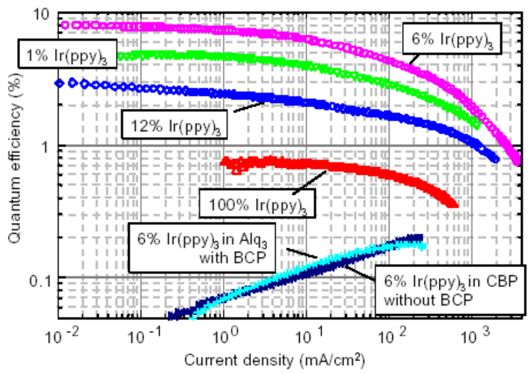

Ref. M. A. Baldo, C. Adachi, and S. R. Forrest, Phys. Rev. B **62**, 10967 (2000)

T – T Annihilation: Steady-state solution

$$\frac{dn_T}{dt} = 0 \qquad \frac{1}{2}k_T n_T^{\,2} + \frac{n_T}{\tau} - \frac{J}{gd} = 0$$

(근의 공식)

$$n_T = \frac{-\frac{1}{\tau} + \sqrt{(\frac{1}{\tau})^2 + \frac{2Jk_T}{qd}}}{k_T} = \frac{1}{k_T\tau}\left[-1+\sqrt{1+\frac{2Jk_T\tau^2}{qd}}\right] = \frac{1}{k_T\tau}\left[-1+\sqrt{1+\frac{8J}{J_T}}\right] \qquad (\because \frac{k_T\tau^2}{4qd} = J_T^{-1})$$

Light emission intensity $L = \frac{n_T}{\tau}$ QE : $\eta = \frac{L}{J} = \frac{n_T}{J\tau}$

η_0 : $k_T = 0$ 인 경우, 즉 , T-T annihilation이 없는 경우이므로 $\frac{n_T}{\tau} = \frac{J}{gd}$

$$\therefore \eta_0 = \frac{L}{J} = \frac{\frac{n_T}{\tau}}{J} = \frac{1}{qd}$$

$$\frac{\eta}{\eta_0} = \frac{qd}{k_T\tau^2 J}\left[-1+\sqrt{1+\frac{8J}{J_T}}\right] = \frac{J_T}{4J}\left[-1+\sqrt{1+\frac{8J}{J_T}}\right]$$

M. A. Baldo, C. Adachi, and S. R. Forrest, Phys. Rev. B **62**,10967 (2000)

Triplet exciton – polaron quenching

$$\frac{d[n_{ex}]}{dt} = -\frac{[n_{ex}]}{\tau} - \frac{1}{2}k_{TT}[n_{ex}]^2 - k_P\left[\frac{\rho_c(j)}{e}\right][n_{ex}] + \frac{j}{ew}$$

$$\frac{\eta(j)}{\eta_0} = \Theta\left[\sqrt{\frac{\Delta^2 + \Gamma k_{TT}}{k_{TT}^2}} - \frac{\Delta}{k_{TT}}\right]$$

$$\Theta = \frac{ew}{\tau j},$$

$$\Delta \equiv \Delta(k_P) = \left(\frac{1}{\tau} + k_P C j^{1/(l+1)}\right)$$

$$\Gamma = \frac{2j}{ew}.$$

	τ [μs]	k_{TT} [10^{-12} cm^3 s^{-1}]	$k_{P,e}$ [10^{-12} cm^3 s^{-1}]	$k_{P,h}$ [10^{-12} cm^3 s^{-1}]	η_0 [%]	w [nm]
TCTA:Ir(ppy)$_3$	(1.58±0.05)	(3±2)	(0.2±0.1)	(0.3±0.2)	15.8	10
NPB:Ir(piq)$_3$	(1.10±0.05)	(1.4±0.6)	(0.7±0.2)	(0.2±0.2)	7.6	19

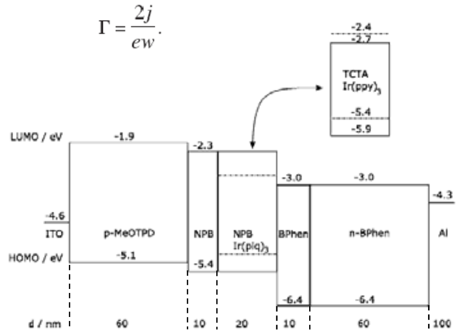

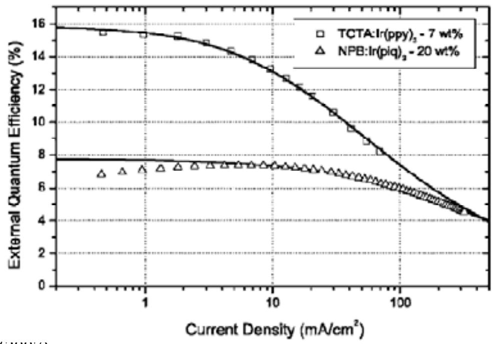

S. Reineke, K. Walzer, and K. Leo, Phys. Rev. B **75**, 125328 (2007)

Spontaneous emission from planar microcavity

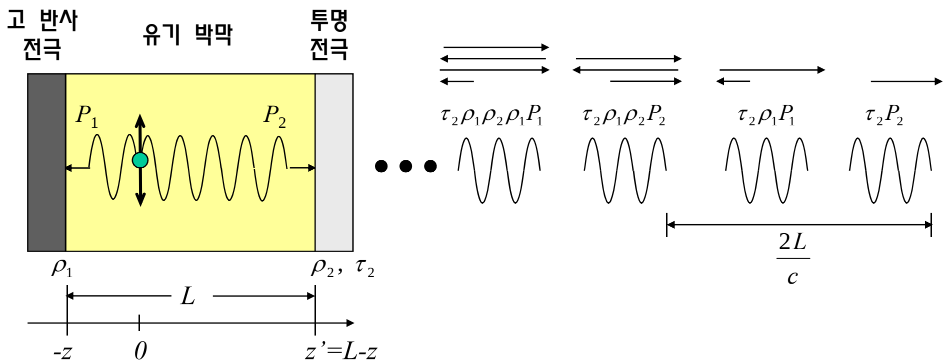

$$E_{L2}(t) = \tau_2 WP(t) + \tau_2\rho_1 WP(t - \frac{2z_1}{c}) + \tau_2\rho_1\rho_2 WP(t - \frac{2L}{c})$$

$$+ \tau_2\rho_1\rho_1\rho_2 WP(t - \frac{2z_1}{c} - \frac{2L}{c})$$

D. G. Deppe, C. Lei, C. C. Lin, and D. L. Huffaker, J. Modern Optics **41**, 325 (1994)

Spontaneous emission from planar microcavity

$$E_{L2}(\omega) = \frac{\tau_2}{2\pi}\int_{-\infty}^{\infty} \underbrace{WP(t)\exp(i\omega t)dt}_{WP(\omega)} + \frac{\tau_2\rho_1}{2\pi}\int_{-\infty}^{\infty} WP(t-\frac{2z_1}{c})\exp(i\omega t)dt$$

$$+\frac{\tau_2\rho_1\rho_2}{2\pi}\int_{-\infty}^{\infty} WP(t-\frac{2L}{c})\exp(i\omega t)dt$$

$$+\frac{\tau_2\rho_1\rho_1\rho_2}{2\pi}\int_{-\infty}^{\infty} WP(t-\frac{2z_1}{c}-\frac{2L}{c})\exp(i\omega t)dt + ...$$

$$E_{L2}(\omega) = \tau_2 WP(\omega) + \tau_2\rho_1 e^{i\frac{2\omega z_1}{c}} WP(\omega) + \tau_2\rho_1\rho_2 e^{i\frac{2\omega L}{c}} WP(\omega)$$

$$+\tau_2\rho_1\rho_2\rho_1 e^{i\frac{2\omega z_1}{c}+i\frac{2\omega L}{c}} WP(\omega) + \tau_2\rho_1\rho_2\rho_1\rho_2 e^{i\frac{4\omega L}{c}} WP(\omega) + ...$$

$$=\tau_2 WP(\omega)[1+\rho_1 e^{i\frac{2\omega z_1}{c}} + \rho_1\rho_2\rho_1 e^{i\frac{2\omega z_1}{c}+i\frac{2\omega L}{c}} + ...$$

$$+\rho_1\rho_2 e^{i\frac{2\omega L}{c}} + \rho_1\rho_2\rho_1\rho_2 e^{i\frac{4\omega L}{c}} + ...\ ]$$

$$E_{L2}(\omega) = \tau_2 WP(\omega)[1+\rho_1 e^{i\frac{2\omega z_1}{c}}\{1+\rho_2\rho_1 e^{i\frac{2\omega L}{c}} + ...\}$$

$$+\rho_1\rho_2 e^{i\frac{2\omega L}{c}}\{1+\rho_1\rho_2 e^{i\frac{2\omega L}{c}} + ...\}]$$

$$1+\rho_2\rho_1 e^{i\frac{2\omega L}{c}} + ... = \frac{1}{1-\rho_2\rho_1 e^{i\frac{2\omega L}{c}}}$$

Spontaneous emission from planar microcavity

$$E_{L2}(\omega) = \tau_2 WP(\omega)\frac{1+\rho_1 e^{i\frac{2\omega z_1}{c}}}{1-\rho_1\rho_2 e^{i\frac{2\omega L}{c}}}$$

Emission spectrum in the forward direction

$$\left|E_{L2}(\omega)\right|^2 = \frac{(1-R_2)[1+R_1+2\sqrt{R_1}\cos(\frac{2\omega n z_1}{c})]}{1+R_1R_2-2\sqrt{R_1R_2}\cos(\frac{2\omega L}{c})}\left|WP(\omega)\right|^2$$

Interference effect (numerator)

Fabry-Perot Resonator (denominator)

$$= \frac{(1-R_2)[1+R_1+2\sqrt{R_1}\cos(\frac{4\pi n z_1}{\lambda})]}{1+R_1R_2-2\sqrt{R_1R_2}\cos(\frac{4\pi n L}{\lambda})}\left|WP(\omega)\right|^2$$

$$|\rho_1|^2 = R_1\ ,|\rho_2|^2 = R_2\ ,|\tau_2|^2 = 1-R_2$$

D. G. Deppe, C. Lei, C. C. Lin, and D. L. Huffaker, J. Modern Optics **41**, 325 (1994)

Radiation mode in top-emitting OLED

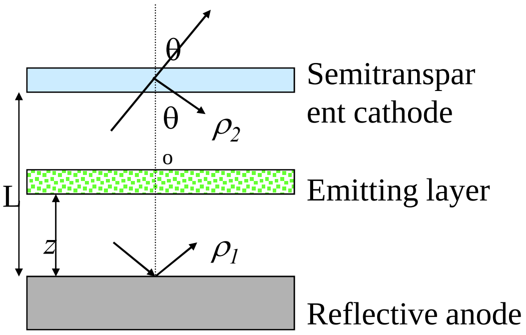

$$I_{ext}^{(s,p)}(\theta,\lambda)=\frac{\left|1+r_1^{(s,p)}\exp(i\frac{4\pi nz\cos\theta_o}{\lambda})\right|^2}{\left|1-r_1^{(s,p)}r_2^{(s,p)}\exp(i\frac{4\pi nL\cos\theta_o}{\lambda})\right|^2}T_2^{(s,p)}I_{\text{int}}^{(s,p)}(\lambda)$$

C. Qiu, H. Peng, H. Chen, Z. Xie, M. Wong, and H. S. Kwok, IEEE Trans. on Electron Dev. 51, 1207 (2004).

Resonant emission from microcavity

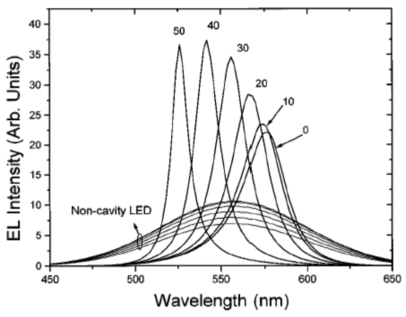

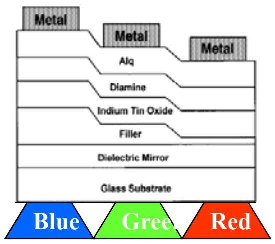

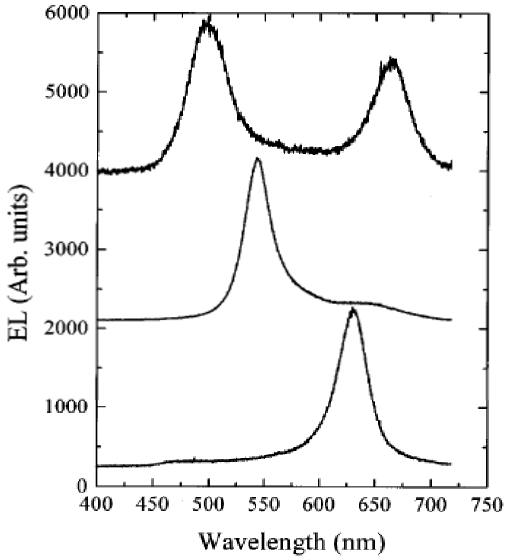

A. Dodabalapur, L. J. Rothberg, R. H. Jordan, T. M. Miller, R. E. Slusher, and J. M. Phillips, J. Appl. Phys. **80**, 6954 (1996).

Radiation mode in top-emitting OLED

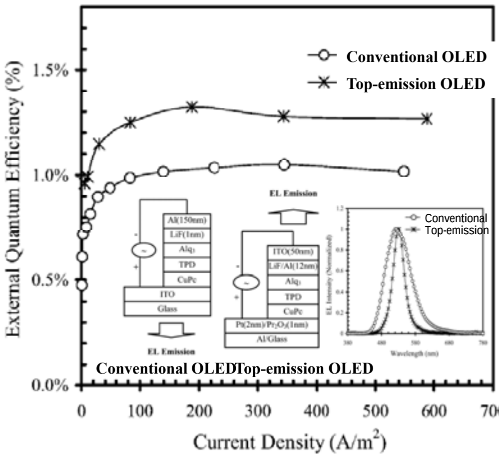

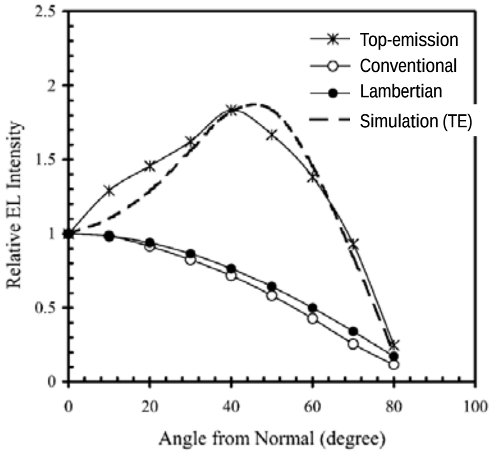

C. Qiu, H. Peng, H. Chen, Z. Xie, M. Wong, and H. S. Kwok, IEEE Trans. on Electron Dev. 51, 1207 (2004).

Organic Semiconductor
EE 4541.617A
2009. 1st Semester

External quantum efficiency of OLED

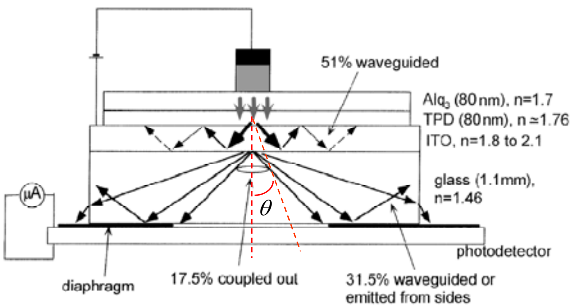

$\sin^{-1}(\frac{n_{substrate}}{n_{organic}}) = \theta_{c2} \le \theta$: ~51%

$\theta_{c1} \le \theta \le \theta_{c2}$: ~31.5%

$\theta \le \theta_{c1} = \sin^{-1}(\frac{n_{air}}{n_{organic}})$: $\eta_C \approx \frac{1}{2n^2_{org}}$ ~17.5 %

G. Gu, DZ Garbuzov, PE Burrows, S. Venkatesh, SR Forrest, ME Thompson, Opt. Lett. 22, 396 (1997)

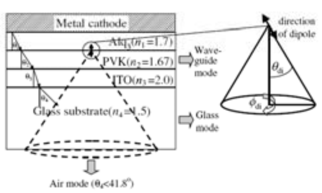

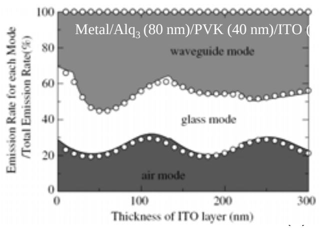

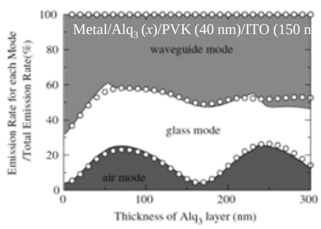

A. Chutinan, K. Ishihara, T. Asano, M. Fujita, S. Noda, Org. Electron. 6, 3 (2005).

Methods of improving out-coupling efficiency

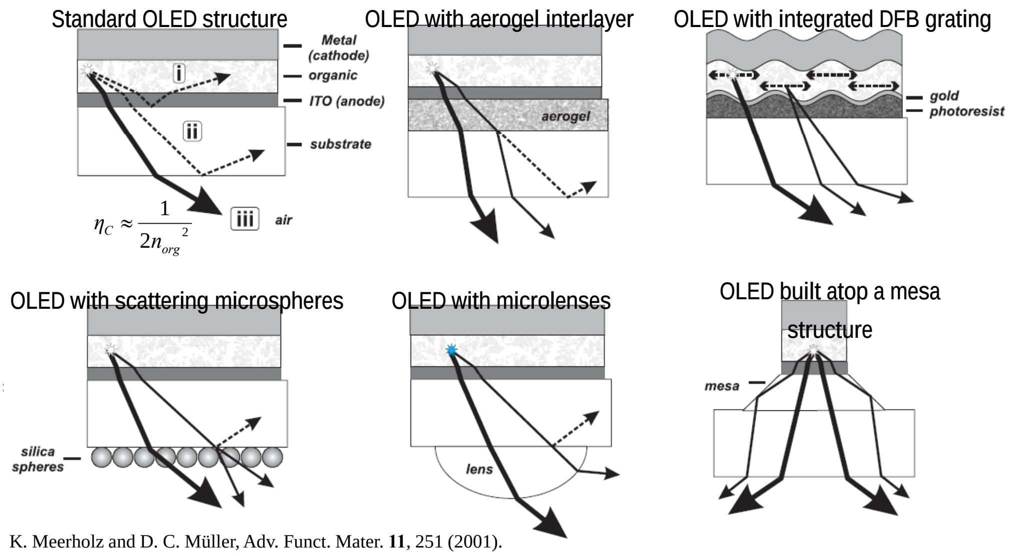

$$\eta_C \approx \frac{1}{2n_{org}^2}$$

K. Meerholz and D. C. Müller, Adv. Funct. Mater. **11**, 251 (2001).

Index matching using a thin aerogel layer

Doubling Coupling-Out Efficiency in Organic Light-Emitting Devices Using a Thin Silica Aerogel Layer
T. Tsutsui, M. Yahiro, H. Yokogawa, K. Kawano, M. Yokoyama, Adv. Mater. **13,** 1149-1152 (2001).

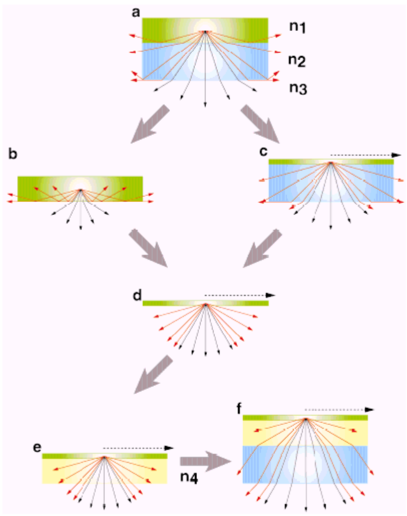

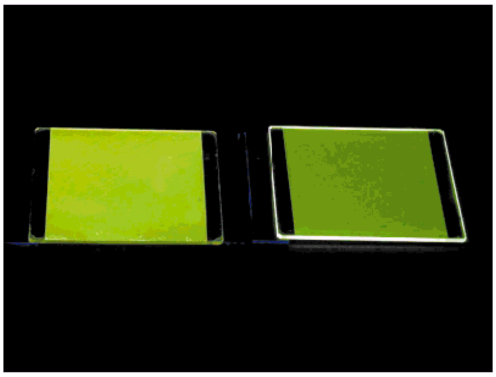

Fig. 3. Photograph of ultrathin emissive layer on glass substrate with (left) and without (right) aerogel spacer layer under UV irradiation. The left picture corresponds to Figure 1f and the right one to Figure 1c. Intense edge emission is observable only in the right sample.

Photonic crystal

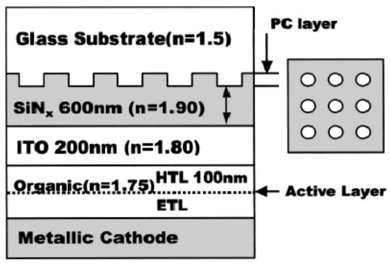

FIG. 1. The layer structure of a PC-OLED with SiN_x and SiO_2/SiN_x PC layers. The specified refractive indices are the wavelength at 530 nm and ETL layer thickness is defined as D_a.

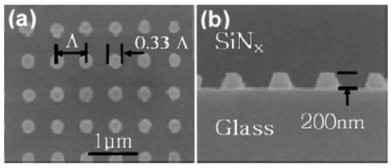

FIG. 4. Scanning electron micrographs: (a) top view and (b) cross-sectional view of the PC-OLED layers.

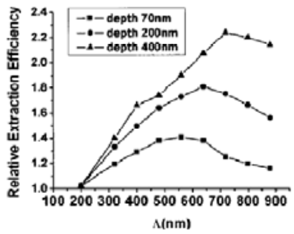

FIG. 3. Extraction efficiencies with respect to the conventional OLED as functions of the lattice constant for three etch depths.

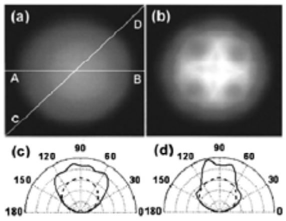

FIG. 5. Far-field intensity profiles. (a) The conventional OLED. (b) The PC-OLED. (c) and (d) Intensity profiles along the horizontal line (A–B) and diagonal line (C–D), respectively. (Dotted lines: conventional OLED, solid lines: PC-OLED.)

Yong-Jae Lee, Se-Heon Kim, Joon Huh, Guk-Hyun Kim, and Yong-Hee Lee, Sang-Hwan Cho, Yoon-Chang Kim, and Young Rag Do, Appl. Phys. Lett. 82, 3779 (2003).

Degradation Processes

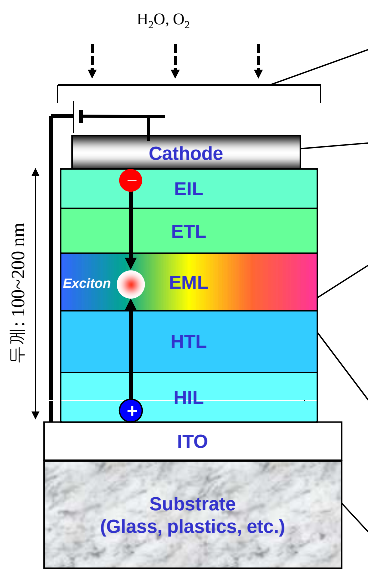

• Encapsulation
- Permeation of H_2O and O_2, etc.

• Ambient environment:
- Temperature, moisture, and UV light, etc.

• Joule heating, etc.

Cathode
- Delamination of metal (Peel-off)
- Corrosion & oxidation; O_2, H_2O
- Diffusion of metals such as Ca, Al, etc.

Electrode Interfaces
- Interfacial degradation
  → Changes in injection efficiency
- Formation of oxide layer: injection barrier
- Electrochemical reaction with organic layers
- Degradation of PEDOT:PSS
- Degradation of p-, n-doped layers, etc.

Organic layers
- Degradation of organic materials
- Photo-oxidation
- Morphological changes (Crystallization):
  change of mobility, trap distribution
  → change in e-h balance, etc.
- Interdiffusion between org./org. interfaces
- Trap formation at org./org. interfaces

Anode
- ITO inhomogeneity: injection barrier
- Oxygen or In diffusion → Degradation of organic layers
- Dust, particles, etc.

Joule heating

Real-Time Observation of Temperature Rise and Thermal Breakdown Processes in Organic LEDs Using an IR Imaging and Analysis System

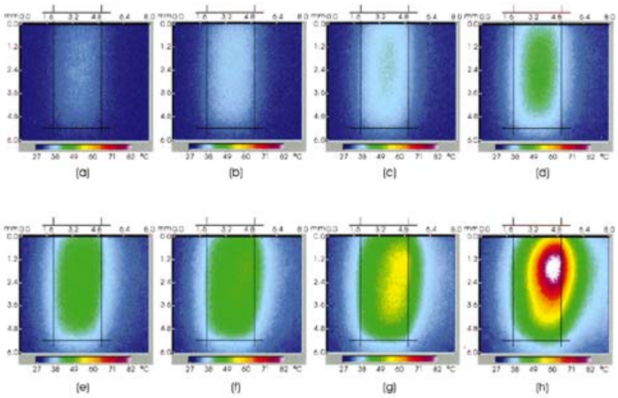

Fig. 3. Surface temperature images of OLEDs: a) 18 V, 32 mA/cm², 35 °C; b) 20 V, 49 mA/cm², 37 °C; c) 22 V, 66.5 mA/cm², 40 °C; d) 24 V, 87.7 mA/cm², 43 °C e) 26 V, 108 mA/cm², 46 °C; f) 28 V, 125 mA/cm², 49 °C; g) 30 V, 146.5 mA/cm², 55 °C; h) 33 V, 220 mA/cm², 86 °C.

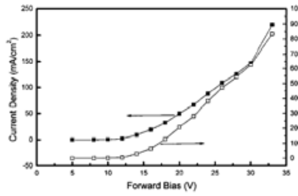

Fig. 1. The *V–I–B* characteristics of the OLEDs.

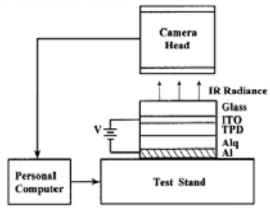

Fig. 2. Experimental set-up used for measurement of temperature.

Xiang Zhou, Jun He, Liang S. Liao, Ming Lu, Xun M. Ding, Xiao Y. Hou, Xiao M. Zhang, Xiao Q. He, and Shuit T. Lee, Adv. Mater. 12, 265 (2000)

Organic Semiconductor
EE 4541.617A
2009. 1st Semester

Impact of Joule heating on the brightness homogeneity of OLEDs

Brightness distribution of a device having an active area of 15 cm² at a current density of 33.3 mA/cm².

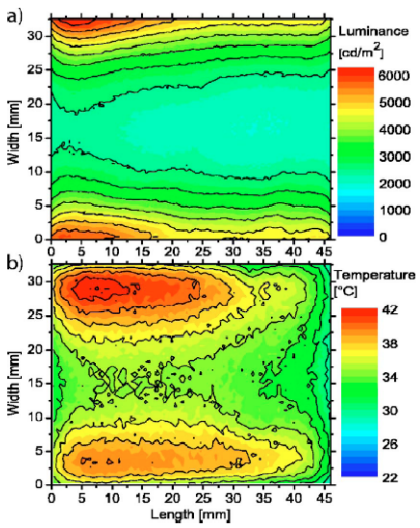

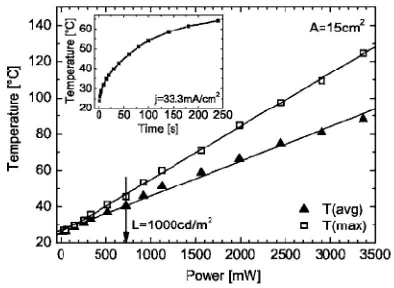

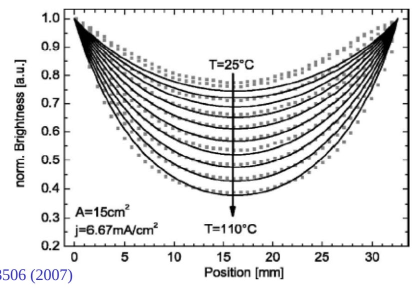

C. Gärditz, A. Winnacker, F. Schindler, R. Paetzold, Appl. Phys. Lett. **90**, 103506 (2007)

Coulombic degradation scaling law

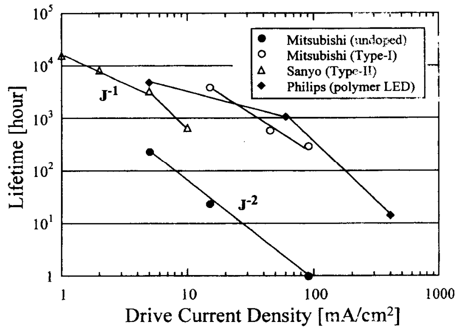

Y. Sato, *Electroluminescence I*, edited by G. Mueller (Academic Press, San Diego, 2000) pp. 209-254.

$$\tau \propto J^{-n}; \quad L_o{}^n \tau = \text{constant}$$

$$\mathrm{L_0}^n \times \mathrm{t}_{1/2} = \text{constant.} \quad \mathrm{n} = 1.7$$

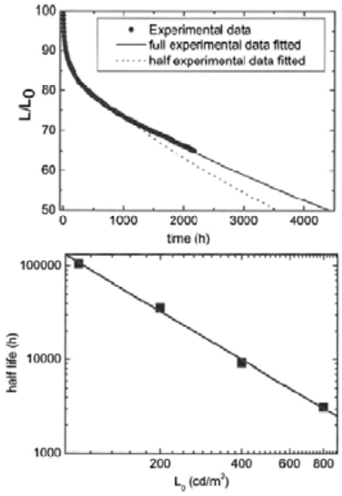

C. Féry, B. Racine, D. Vaufrey, H. Doyeux, and S. Cinà, Appl. Phys. Lett. **87**, 213502 (2005)

Degradation due to H_2O permeation

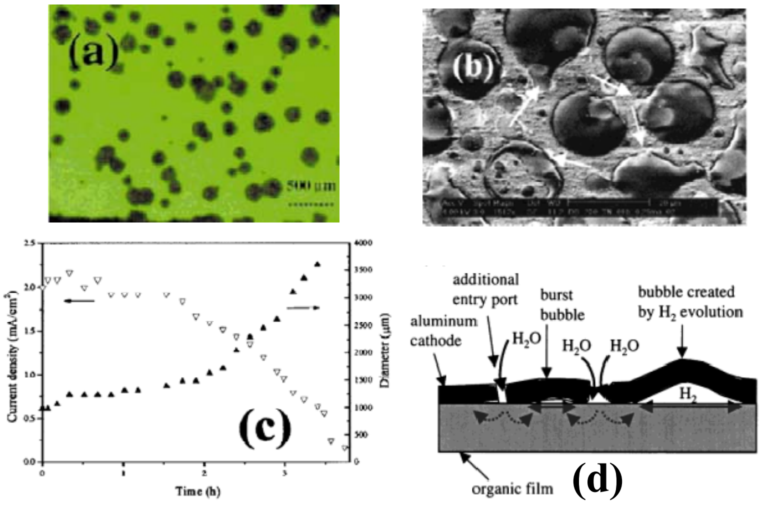

M. Schaer, F. Nüesch, D. Berner, W. Leo, and L. Zuppiroli, Adv. Funct. Mater. 11, 116 (2001).

Encapsulation

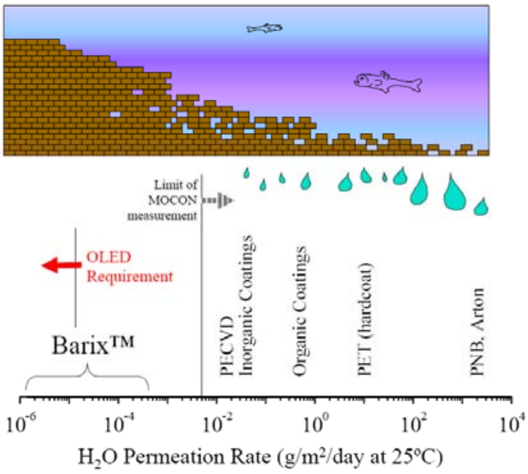

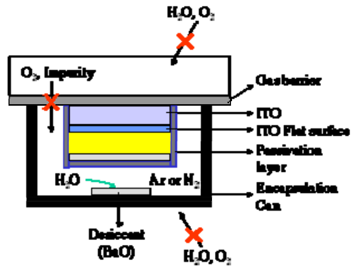

Rigid OLED Architecture:

Pioneer Patent EP 0 776 147 A1

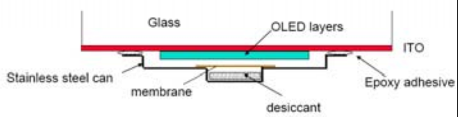

P. E Burrows, G. L. Graff, M. E. Gross, P. M. Martin, M. Hall, E. Mast, C. Bonham, W. Bennett, L. Michalski, M. Weaver, J. J. Brown, D. Fogarty, L. S. Sapochak, Proceedings of SPIE **4105**, 75 (2001).

Thin film encapsulation

- **Inorganic:**
- Aluminum oxide deposited by DC reactive sputtering
- Thickness 30-100 nm
- **Organic:**
- Monomer mixture deposited in vacuum
- Non-conformal deposition: Liquid-Vapor-Liquid- (UV curing)-So
- Thickness 0.25 – several mm
- **4-5 polymer / inorganic pairs (dyads) for encapsulation**

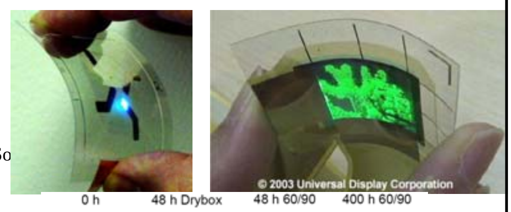

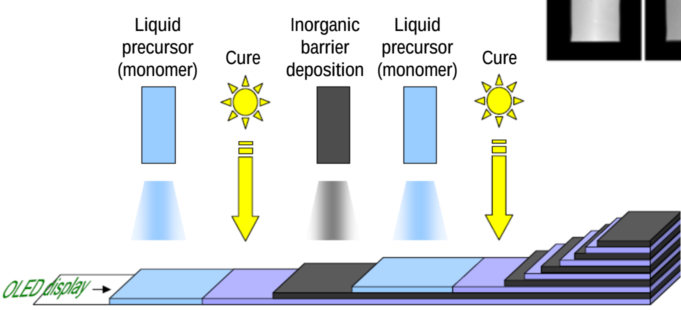

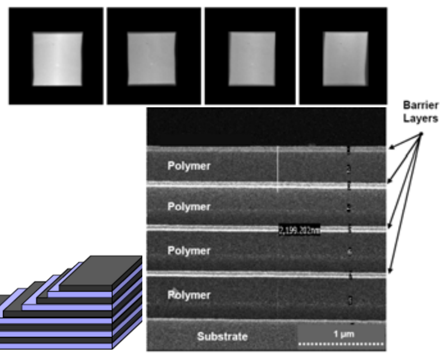

L. L. Moro, T. A. Krajewski, N. M. Rutherford, O. Philips, R. J. Visser, M. E. Gross, W. D. Bennett, and G. L. Graff, Proceedings of SPIE **5214**, 83 (2004).

Methods of Full Color Display Fabrication

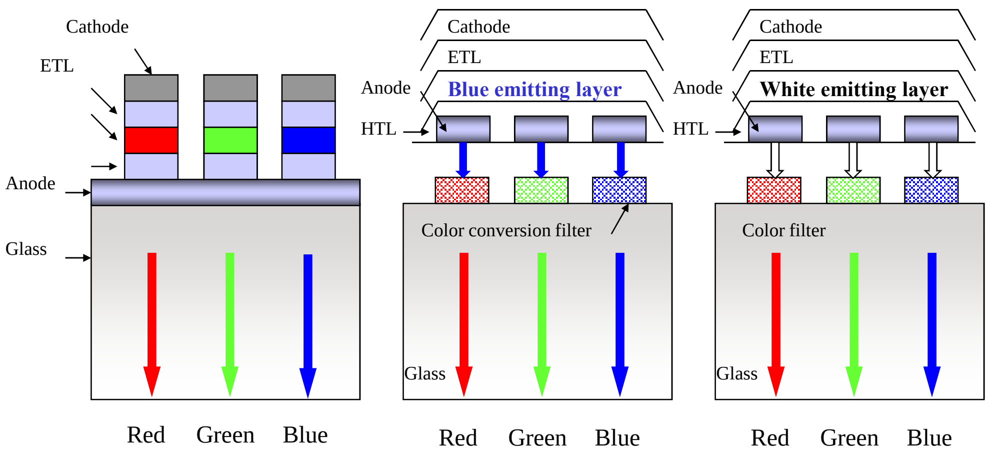

Comparison of OLED color patterning methods

Items	Evaporation (Precision Shadow Mask)	Ink-Jet Printing	Laser-Induced Thermal Imaging (LITI)
Materials	Molecular Materials Only 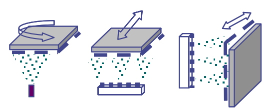	Polymer (LEP) 	Polymer (LEP) Molecular Materials Hybrids (Blend) 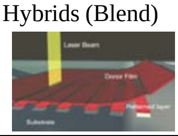
Printing Accuracy	± 15㎛	± 15㎛	± 2.5㎛
Resolution	~180ppi	~150ppi	~300ppi
Aperture Ratio (Top Emission)	40~50%	~60%	70~80%
Materials Usage	-	Smallest	-
Glass Size	730x460mm (~2005)	730x920mm	730x920mm (~2005)
Machine Price	Very Expensive	Cheapest	Middle

Source: Samsung SDI, FPD int. 2004

PMOLED

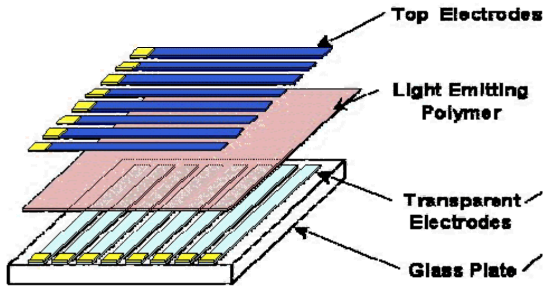

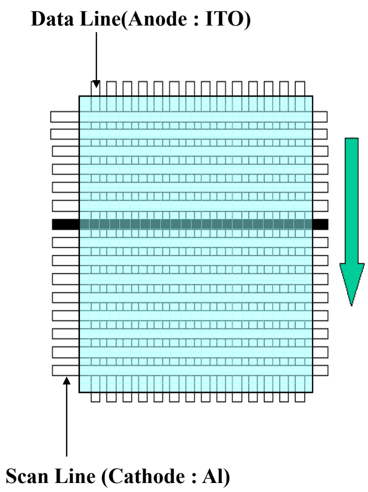

AMOLED

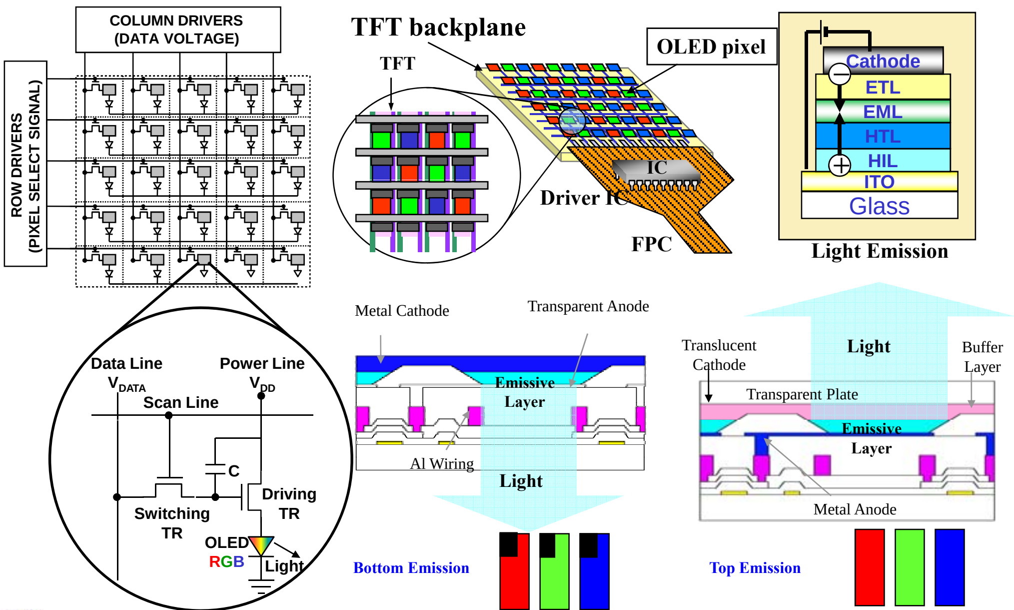

AM OLED Process Map

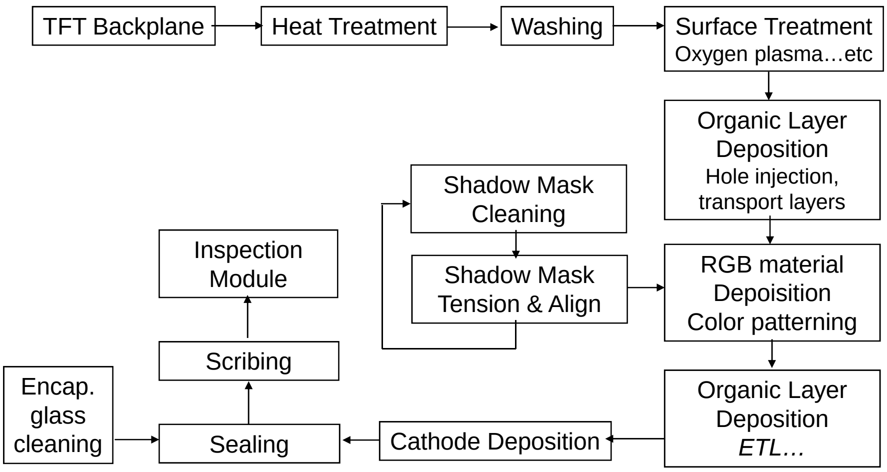

Source: B. D. Chin (KIST), IMID 2006